Proceedings of the ASME 2026 International Technical Conference and Exhibition on Packaging and Integration of Electronic and Photonic Microsystems
InterPACK2026
October 26-29, 2026, San Diego, California

IPACK2026-194172

EXPERIMENTAL INVESTIGATION OF FLOW BOILING IN MICROCHANNEL COLD PLATES FOR DATA CENTER TWO-PHASE COOLING

Qingyang Wang
Accelsius
Austin, TX
qwang@accelsius.com

Trevor A. Whitaker
Accelsius
Austin, TX

Akshith Narayanan
Accelsius
Austin, TX

Richard W. Bonner
Accelsius
Austin, TX

ABSTRACT

The rapid growth in AI computing demand is driving substantial increases in processor and rack-level power densities, creating significant challenges for thermal management of modern data centers. Advanced cooling technologies are therefore required to support the continued evolution of high-performance processors and server architectures. Pumped two-phase direct-to-chip cooling has emerged as a promising approach, offering advantages in thermal performance and energy efficiency by leveraging the high heat transfer coefficients associated with liquid-vapor phase-change processes.

Although future processors operating at substantially higher heat fluxes may require cold plate designs specifically optimized for phase-change heat transfer through capillary-assisted structures, surface enhancements, or innovative liquid supply and vapor removal strategies, current processor heat flux levels remain within a range that can be effectively managed by conventional microchannel cold plates employing flow boiling. In particular, skived-fin microchannel cold plates are widely adopted in data center cooling applications due to their cost-effective manufacturability, mature fabrication processes, broad vendor availability, and robust thermal performance.

While classical correlations for heat transfer and pressure drop of flow boiling in microchannels can provide useful guidance for cold plate design, these correlations are generally developed from limited experimental data and are only applicable for a narrow range of operating conditions, specific flow regimes, or selected working fluids. Therefore, experimental investigation remains essential for understanding the thermohydraulic behavior of two-phase microchannel cold plates and for guiding their design and optimization, especially under realistic data center operating conditions. In this study, the thermohydraulic performance of skived-fin microchannel cold plates designed for a representative processor package is experimentally investigated using R515B as the working fluid. A series of cold plates with systematically varied channel geometries were fabricated, and their performance was measured across a range of conditions. A maximum footprint heat transfer coefficient of over 170 kW/m^{2}K was obtained. The effects of flow rate, heat flux, and channel geometry on the footprint heat transfer coefficient and pressure drop are analyzed and discussed, and the results are compared with an existing predictive model. This work provides practical insights into the parametric optimization of microchannel cold plate designs, supporting the development of efficient two-phase cooling solutions for next-generation high-performance data centers.

Keywords: flow boiling, two-phase cooling, direct-to-chip, cold plate, data center, thermal management

NOMENCLATURE

2P	two-phase
CFD	computational fluid dynamics
CP	cold plate
DTC	direct-to-chip
FEA	finite element analysis
HTC	heat transfer coefficient
MARE	mean absolute relative error
MRE	mean relative error
PCM	phase change material
RMSRE	root mean square relative error
TC	thermocouple
TIM	thermal interface material
TTV	thermal test vehicle

Copyright © 2026 by ASME

1. INTRODUCTION

The rapid increase in AI and high-performance computing workloads is driving significant increases in processor and rack-level power densities in modern data centers. Conventional air cooling and even single-phase liquid cooling approaches face increasing challenges in maintaining acceptable junction temperatures and energy efficiency. Consequently, advanced thermal management solutions are required to enable the continued scaling of next-generation processors and server architectures while meeting constraints on performance, reliability, and scalability.

Cold plate based pumped two-phase (2P) direct-to-chip (DTC) cooling has attracted considerable attention due to its ability to leverage latent heat during phase change, resulting in high heat transfer coefficients (HTCs) [1]. By utilizing flow boiling within compact cold plates, 2P DTC systems can remove large heat fluxes with relatively small coolant flow rate, offering potential advantages in thermal performance and system efficiency for future data center thermal management [2, 3].

Despite the outstanding performance and promising potential of innovative surface structures and/or fluid management designs specifically optimized for phase-change heat transfer [4, 5], microchannel cold plates are widely employed in 2P cooling due to their manufacturing simplicity and the sufficiently high heat transfer performance of microchannel flow boiling. In particular, skived-fin microchannel cold plates have gained broad adoption in data center applications because of their cost-effective manufacturing, mechanical robustness, and compatibility with existing supply chains [6, 7]. High power and high heat flux dissipation have been experimentally demonstrated using skived-fin cold plates for 2P DTC cooling [8-12].

Although microchannel flow boiling has been studied extensively [13-15], predictive modeling of thermohydraulic performance remains challenging. Existing correlations are often developed from limited experimental datasets and are typically valid only over a narrow range of operating conditions, flow regimes, and working fluids [16, 17]. In practical cold plate configurations, the interaction between channel geometry, heat flux, mass flux, and phase distribution can lead to complex thermohydraulic behavior that deviates from these models. Furthermore, relatively few existing studies have focused on geometries and operating conditions representative of practical data center application conditions, particularly for state-of-the-art skived-fin designs with narrow and high-aspect-ratio channels [18]. As a result, there remains a need for systematic experimental investigations under application-relevant conditions to better understand the performance of skived-fin microchannel cold plates and to support their design optimization.

In this work, an experimental investigation is conducted to evaluate the thermohydraulic performance of skived-fin microchannel cold plates for data center 2P DTC cooling applications. The performance is characterized at steady-state; investigation of transient responses to rapid power variations is beyond the scope of the present study and is recommended for future work. A maximum footprint HTC of over 170 kW/m^{2}K was obtained experimentally. The effects of key geometric and operating parameters on heat transfer and pressure drop are examined, and the results are compared with an existing predictive model. The findings provide experimentally grounded insights into the parametric design and optimization of microchannel cold plates for high-performance data center cooling.

2. EXPERIMENTAL

2.1. Experimental System

The experimental system used in this work is essentially a lab-scale two-phase coolant distribution unit (CDU), similar to the ones used in Refs. [8-10]. Figure 1 shows the schematic of the test system, which has a refrigerant circulation loop with R515B as the working fluid, including a reservoir (McMaster-Carr), a gear pump (Micropump GJ-N27), a test section, and a brazed-plate heat exchanger (HTG030B) as a condenser. A custom-built dry cooler (an air-cooled water circulator) with a water circulating loop is connected to the condenser, where room temperature air is used to cool the circulating water, and the chilled water flows through the brazed-plate heat exchanger to condense the refrigerant in the test loop.

The test section includes a cold plate being tested, which is attached to a thermal test vehicle (TTV) with a PCM-based thermal interface material (TIM). The cold plate is connected to the loop through two pairs of quick-disconnect couplings for ease of maintenance and servicing. A clamp-on ultrasonic flow meter (Keyence FD-X series), two absolute pressure sensors (Omega PX309), two T-type thermocouples, and a differential pressure sensor (Omega PX409) are used to measure the inlet volumetric flow rate through the cold plate, the pressures at the inlet and outlet of the cold plate, the temperatures at the inlet and outlet of the cold plate, and the pressure drop across the cold plate, respectively. An AC power controller (Gefran GFX4-IR) provides heat input into the cartridge heaters inserted into the

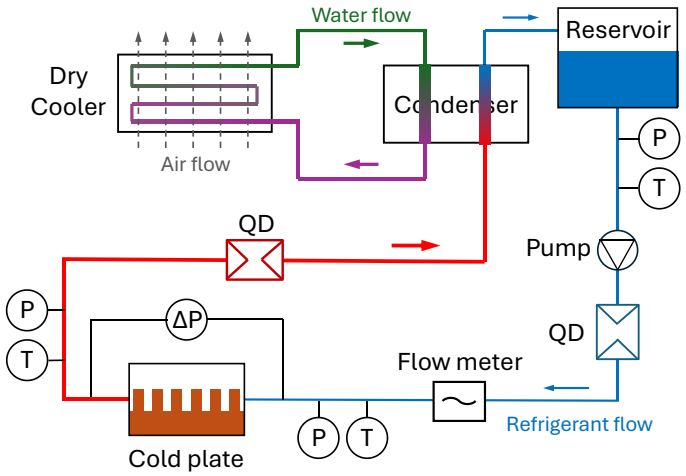


FIGURE 1: Schematic of the experimental system.

Copyright © 2026 by ASME

TTV, and a data acquisition unit (Keysight DAQ970A) collects measurements from the sensors implemented within the loop at a frequency of 1 Hz. An in-house developed LabVIEW program is used to control the fluid pump speed, TTV heating power, and data acquisition. For each steady state condition, the measurements of temperature, pressure, differential pressure, and flow rate are all averaged over a 10-second period.

2.2. TTV and Cold Plates

The TTV used in this work is designed to match the logic die area of a specific processor package not to be named in this work. The TTV is made of copper C110, and includes a base portion to house the cartridge heaters and a neck portion to develop one-dimensional conduction and contact the cold plate, as shown in Figure 2(a). The TTV top surface has a heated area of 26×35 mm^2 to interface with the cold plate. A thermocouple hole is positioned 6.5 mm below the top surface, and a T-type thermocouple is inserted into the hole with its tip positioned directly below the center of the heated surface. The thermocouple measurement is used to obtain TTV surface temperature based on one-dimensional heat conduction analysis. The base portion contains four 0.25" diameter holes drilled horizontally to house four cartridge heaters. The cartridge heaters each have 500 W of rated power, corresponding to a maximum TTV power of 2000 W and a maximum heat flux of 220 W/cm^2. The copper TTV body is insulated with PEEK to reduce heat loss. Mica ceramic sheets are placed between the base portion of the TTV body and the PEEK insulation, to offer high-temperature insulation capability and prevent overheating and softening of the PEEK, as shown schematically in Figure 2(b).

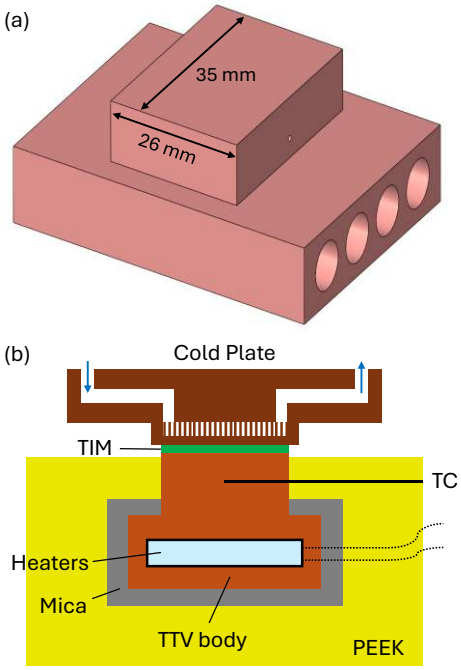


FIGURE 2: (a) 3D model of the TTV body. (b) Schematic of the TTV/cold plate assembly.

Microchannel cold plates are designed to have a pedestal whose size is slightly larger than the TTV heated area size. The cold plate is manufactured by brazing multiple parts together, in which the pedestal part consists of a base plate with microchannels on top formed by a skived fin array. The fin array covered area matches the TTV heated area. Eight cold plates are investigated in this work, with mostly identical design parameters except the different skived fin geometries. The tips of the skived fins are brazed to the roof to provide mechanical support and prevent fluid bypassing. The fins (and channels) are arranged so that the axial direction of the channels is parallel to the short edge of the TTV surface, and the channels are arranged in a pass-through flow configuration, i.e., the effective flow length of the microchannels is 26 mm. The vendor-measured geometrical parameters of the eight different cold plates are listed in Table 1.

TABLE 1: GEOMETRIC PARAMETERS OF THE COLD PLATE SAMPLES USED IN THIS WORK

CP ID	Channel Height (mm)	Channel Width (mm)	Wall Thickness (mm)	Skiving Pitch (mm)
#1	1.271	0.148	0.093	0.241
#2	1.267	0.146	0.094	0.240
#3	1.701	0.104	0.089	0.193
#4	1.778	0.137	0.101	0.238
#5	1.793	0.167	0.133	0.300
#6	1.714	0.219	0.178	0.397
#7	2.739	0.102	0.084	0.186
#8	2.730	0.127	0.112	0.239

2.3. Data Reduction

For each given steady state condition, the measured properties include the inlet and outlet temperatures of the cold plate T_{in} and T_{out}, the inlet and outlet pressures of the cold plate P_{in} and P_{out}, the pressure drop across the cold plate ΔP, the inlet liquid volumetric flow rate $\dot{V}$, the TTV thermocouple temperature T_{TC}, and the supplied heating power Q (from current and voltage measurement). The inlet and outlet pressure measurements are redundant and not used for data processing.

The heat transfer performance of the cold plate is represented using a footprint-based effective HTC, which is obtained based on one-dimensional heat transfer assumption. The heat flux is obtained assuming all the supplied heat conducts upward and is dissipated by the cold plate,

$$q'' = \frac{Q}{A} \quad (1)$$

Copyright © 2026 by ASME

where A is the TTV heated surface area. The TTV surface temperature (or case temperature, T_{case}) can be obtained from the thermocouple measurement,

$$T_{case} = T_{TC} - q'' \frac{\delta}{k_{Cu}} \quad (2)$$

in which k_{Cu} is copper thermal conductivity, and δ = 6.5 mm is the distance of the thermocouple hole below the TTV surface. The flux-based area-specific case-to-outlet thermal resistance of the cold plate [19] is obtained as

$$R_{th} = \frac{T_{case} - T_{out}}{q''} \quad (3)$$

The case-to-outlet thermal resistance includes contributions from TIM, base plate conduction, boiling heat transfer, and two-phase pressure drop [19]. The TIM used in this work is assumed to have a thermal resistance of R_{TIM} = 6 mm^{2}K/W for all tests according to the TIM product datasheet, although the actual resistance could vary between different tests. The exact experimental value of R_{TIM} and its variation among different experiments are difficult to capture directly with the current test setup. Nevertheless, the same TIM and mounting/testing procedure were used for all cold plates, so that the uncertainties associated with R_{TIM} as well as other propagating components are expected to affect the absolute HTC values more strongly, rather than the relative parametric trends. Therefore, the reported results in this work are intended to compare cold plate performance under consistent conditions and provide guidance for future cold plate optimization.

The effective footprint HTC is finally obtained as

$$\text{HTC} = \left(R_{th} - R_{TIM} - \frac{t_{base}}{k_{Cu}}\right)^{-1} \quad (4)$$

where t_{base} is the cold plate base plate thickness. The effective footprint HTC serves as a black-box-type parameter for cold plate performance characterization and incorporates the combined effects of inlet subcooling, surface area enhancement, fin efficiency, boiling performance, and cold plate two-phase pressure drop [20]. It represents the global footprint-area-averaged cold plate performance in a given system, and does not contain information related to local HTC variations. In this work, the apparent subcooling of the cold plate at all testing conditions remained below 5 °C, indicating dominance of two-phase heat transfer over subcooled single-phase convection.

The thermodynamic quality of the two-phase mixture at the exit of the cold plate is obtained by taking into account the inlet subcooling, where the cold plate outlet temperature is assumed to be the constant saturation temperature along the boiling segment of the channels [19].

$$x_{out} = \frac{Q - \dot{V}\rho_l c_p (T_{out} - T_{in})}{\dot{V}\rho_l h_{fg}} \quad (5)$$

in which ρ_l, c_p, and h_{fg} are the liquid density, liquid specific heat capacity, and latent heat, respectively. This exit quality represents the averaged global value at the cold plate outlet, and the channel outlet local qualities can differ and scatter, but are beyond the scope of this work.

3. RESULTS AND DISCUSSION

3.1. Heat Transfer Characteristics

For each cold plate, heat transfer experiments are conducted under multiple nominal flow rate conditions: 0.7 (for CP #3 and #4 only), 1.0, 1.5, and 2.0 L/min. For each given inlet flow rate, the heating power is incrementally applied up to the maximum TTV power capacity of 2000 W. For each power step, the measurements are taken and averaged after steady state condition is reached. In general, the eight cold plates exhibit qualitatively similar thermohydraulic behavior. In this section,

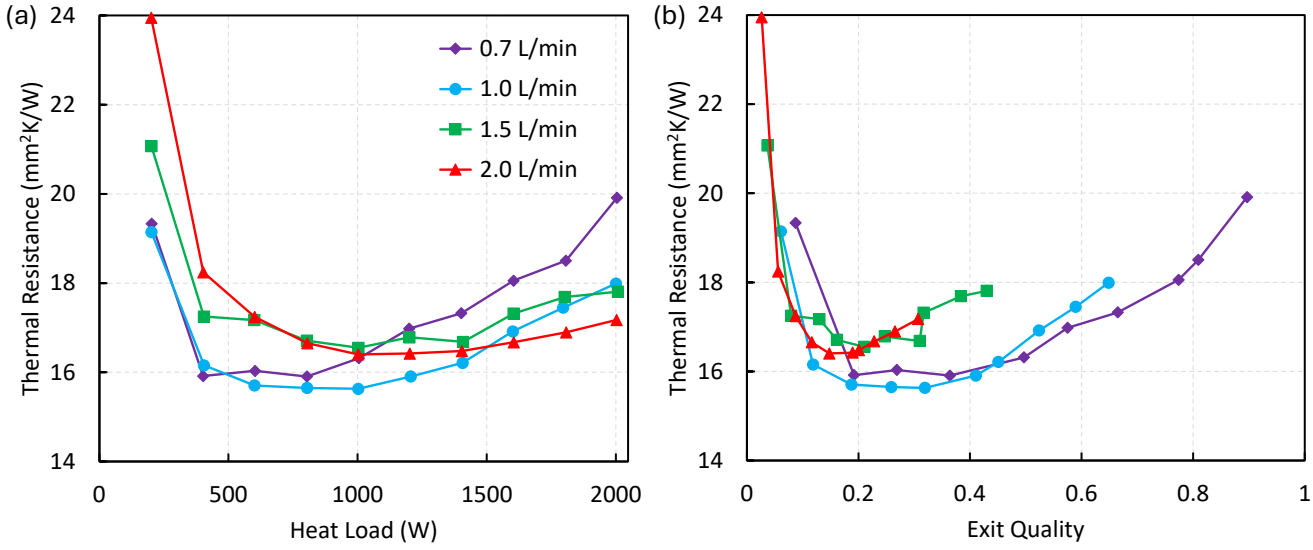


FIGURE 3: Heat-flux-based area-specific case-to-fluid thermal resistance as a function of (a) heat load and (b) cold plate exit quality for CP #3 under different nominal inlet flow rate conditions.

Copyright © 2026 by ASME

CP #3 is used as an example due to its high HTC achieved, and its heat transfer characteristics are discussed below.

Figure 3(a) shows the thermal resistance as a function of heat load, for the four nominal flow rate conditions. The actual flow rates were measured as 0.70±0.03, 1.01±0.03, 1.49±0.05, and 2.04±0.06 L/min, respectively. For all four curves, with increasing heat load, the thermal resistance initially decreases at low power conditions, reaches a minimum at ~16 mm^2K/W, and then increases at higher power conditions. The observed trend is consistent with our previous experimental results [10, 11]. The initial decrease at low power can be attributed to the gradually developing boiling heat transfer and the reduction of single-phase contribution, and the following increase at high power might be attributed to the heat transfer deterioration induced by potential occurrence of dryout incipience [21], flow instabilities, or other mechanisms.

Figure 3(b) plots the thermal resistance as a function of cold plate exit quality. The thermal resistance trend is more clearly displayed, showing initial decrease and later increase with the exit quality, further corroborating the explanation above. Notably, the minimum resistance quality, defined as the exit quality at which the curve reaches the minimum thermal resistance, decreases with increasing flow rate: for 0.7 and 1.0 L/min curves, the minimum resistance occurs at an exit quality of 0.3~0.4; for 1.5 L/min, the minimum resistance quality is ~0.2; and for 2.0 L/min, it is ~0.15. This indicates earlier occurrence of heat transfer deterioration for higher flow rate conditions. However, the present work only captures the cold plate global performance and does not include local wall temperature mapping or flow visualization, and therefore, the local mechanisms causing the global two-phase heat transfer deterioration are hypothesized and not validated.

In Figure 3(b), the low flow rate curves (0.7 and 1.0 L/min) converge across most of the tested range except with slight variation at very low exit quality conditions where subcooled single-phase contribution is significant and boiling is not yet fully developed. Similar convergence is also seen for high flow rate curves (1.5 and 2.0 L/min) after reaching minimum resistance quality. Under fully developed boiling conditions, the convergence of thermal resistance curves with respect to quality instead of heating power (or heat flux) suggests convective boiling dominant regime. For either low flow rate group or high flow rate group, different inlet flow rates yield similar convective boiling performance at a given quality, which can be attributed to the dominance of channel confinement effect in dictating liquid film thickness and thus heat transfer performance [18].

Figure 4(a) plots the effective footprint HTC as a function of heat flux for the four flow rate conditions. Higher flow rate yields lower HTC at low heat flux conditions, due to the larger subcooled single-phase contribution which suppresses nucleation and boiling development [10]. A high footprint HTC of >120 kW/m^2K is achieved at high heat flux exceeding 200 W/cm^2, and a maximum footprint HTC over 170 kW/m^2K is recorded for 1.0 L/min flow rate at ~100 W/cm^2. Figure 4(b) shows the HTC as a function of exit quality, again showing the respective convergence of the low flow rate curves and the high flow rate curves. Figure 4 indicates that the high HTC value is attainable under widely different flow rate and heat flux conditions. This will enable highly efficient cold plate design for processors having multiple zones with different heat fluxes, without having to treat different zones with different structures. Moreover, during numerical simulation of a two-phase cold plate, instead of relying on highly computationally expensive CFD, a conduction-based FEA analysis can be used for quick turnaround design iterations, where the HTC value of ~140 kW/m^2K can be conservatively used as the internal boundary condition between the wall and the fluid domain for the microchannel covered surface.

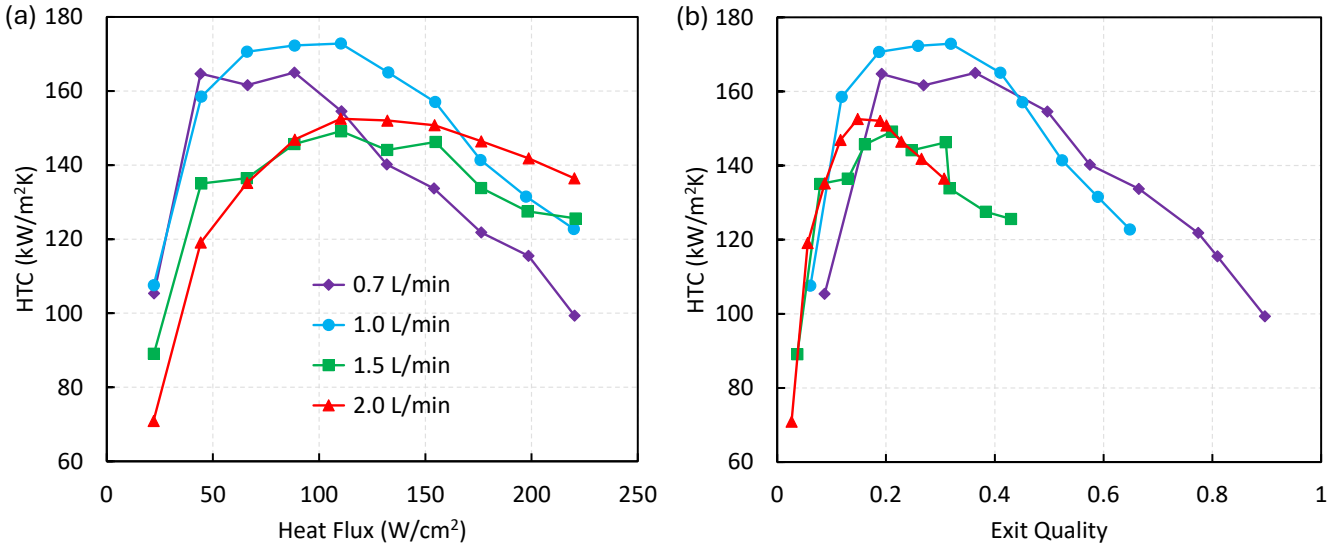


FIGURE 4: Footprint HTC as a function of (a) heat flux and (b) cold plate exit quality for CP #3 under different nominal inlet flow rate conditions.

Copyright © 2026 by ASME

It is noted that the plotted HTC value is sensitive to the assumed TIM resistance. The value of 6 mm^{2}K/W reported by the product datasheet is used in the heat transfer analysis. The datasheet value is obtained following ASTM D5470, typically using well-prepared surface conditions and a relatively small heat transfer area. In our practical applications, the relatively larger heat transfer area, non-ideal surface conditions (roughness, flatness, and parallelness), and potential incomplete burn-in of the PCM can all contribute to a higher thermal resistance for the PCM-based TIM. From previous experimental results with thermocouples embedded in both the TTV and the cold plate [12], we have observed that the same TIM can yield much higher R_{TIM} (>15 mm^{2}K/W) when used for a TTV/cold plate combination with large heat transfer area (>35 cm^2). Therefore, although the datasheet value is used to analyze the HTC in this work, the actual R_{TIM} could be larger with an unknown magnitude for the current TTV condition. Consequently, the HTC reported here is used for demonstration of the relative trend instead of high-fidelity performance metric. Higher HTC can be expected if the actual TIM contribution is accurately quantified in future work.

3.2. Effect of Flow Rate

Two sets of experiments are conducted to investigate the effect of flow rate, where the TTV power is set fixed while the flow rates are varied. Figure 5(a) shows the HTC variation with inlet flow rate, under two different heat load (and heat flux) conditions. Given fixed power and heat flux, the HTC increases with flow rate, which can be attributed to enhanced convective boiling provided by higher flow rate. Although the two curves show a monotonic increase of HTC with flow rate, the trend is expected to reverse at sufficiently high flow rates, where single-phase dominance suppresses boiling, as reported in Ref. [10]. However, the current test loop is unable to supply higher flow rate stably and those conditions are thus not tested.

Figure 5(b) plots the same HTC results as a function of the exit quality. If we assume that the HTC decreases with further increased flow rate beyond 2.5 L/min in Figure 5(a), the HTC will decrease with decreasing quality on the left end of the two curves in Figure 5(b), indicating an HTC peak at the exit quality of <0.2. This is different from previous modeling results which estimated the peak HTC to occur with an exit quality of 0.4~0.6 [20]. The discrepancy may be caused by the practical non-uniform distribution of two-phase flow between parallel channels, whereas the model assumed perfect uniformity and analyzed a single channel. The HTC under higher heat flux (red curve) is lower than that under lower heat flux (blue curve), which may be attributed to the earlier occurrence of dryout incipience or flow instabilities as discussed before.

3.3. Effect of Channel Geometry

The effects of channel width and channel height are analyzed in this work. Although the channel hydraulic diameter is commonly used to represent both parameters in microchannel studies, channel width and height are usually directly used in practical design and manufacturing of skived-fin structures. Moreover, the skived fin geometry produces high aspect ratio channels (height ≫ width) such that the hydraulic diameter is approximately equal to twice the channel width. Consequently, the effect of hydraulic diameter is practically captured by the effect of channel width.

The geometric effects are evaluated by comparing the performance of multiple cold plates with either similar channel heights and varying channel widths, or similar channel widths and varying channel heights. For each cold plate, the performance metrics used are the maximum achieved HTC and the maximum pressure drop across all tested conditions. Since

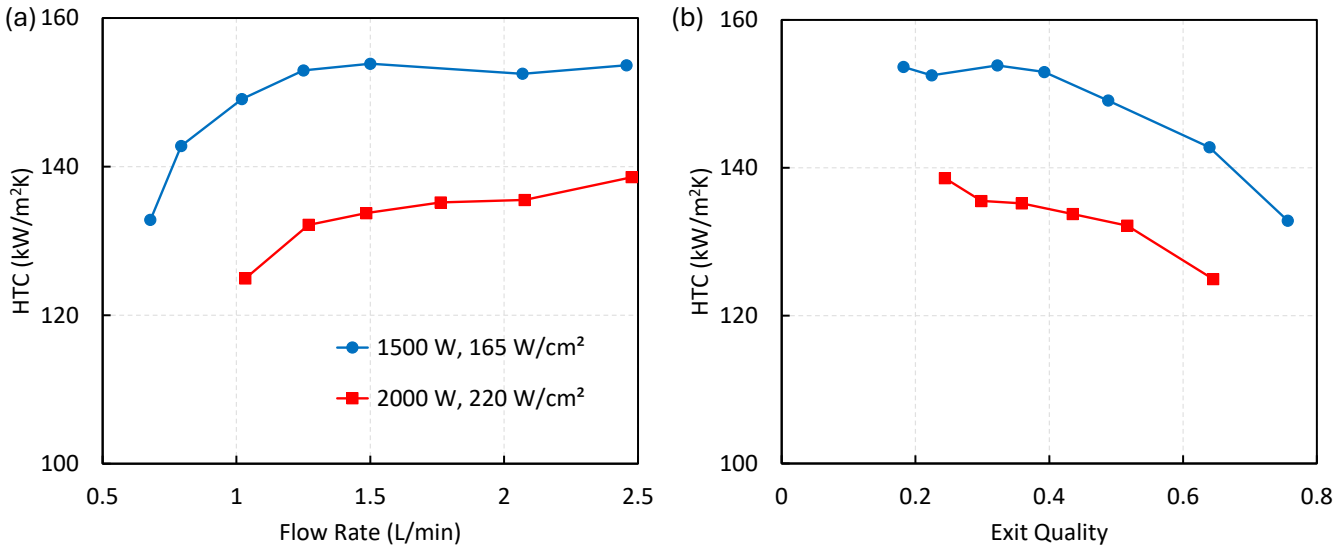


FIGURE 5: Footprint HTC as a function of (a) flow rate and (b) cold plate exit quality for CP #3 under different heat load/heat flux conditions.

Copyright © 2026 by ASME

the pressure drop increases with both flow rate and heat load, the maximum pressure drop occurs at the highest heat flux of 220 W/cm^2 and the largest flow rate of ~2.5 L/min.

As shown in Table 1, CP #3-6 represent a group of designs with similar channel height and different channel width. Figure 6(a) shows the footprint HTC as a function of channel width for this group of cold plates. The maximum HTC decreases monotonically with channel width, which is consistent with previous model prediction [20]. The model also predicts that the trend will reverse with channel width below 0.05 mm [20], which is difficult to manufacture by skiving and is beyond the parameter range investigated in this work. The increase of HTC with decreasing channel width can be attributed to the enhancement of convective boiling, where the liquid film thickness is dictated by the confinement of the channel width [18]. Figure 6(b) plots the maximum pressure drop as a function of channel width for CP #3-6, showing a monotonic decrease trend as expected, since a wider channel given similar channel height provides less flow resistance. Under the same flow rate and power, the pressure drop across the microchannels should scale inversely proportionally to the channel width based on Darcy-Weisbach equation. The curve in Figure 6(b) shows a vertical upward shift from that scaling, indicating that a large fraction of the total pressure drop is contributed by the cold plate inlet/outlet plenums and connectors that are identical between different cold plates and are unrelated to the fin structures.

The channel width obtained from skiving processes has a large manufacturing tolerance relative to the already small nominal channel width. Here, we select CP #1-4 and #7, #8, which have small skiving pitches (approximately 0.19~0.24

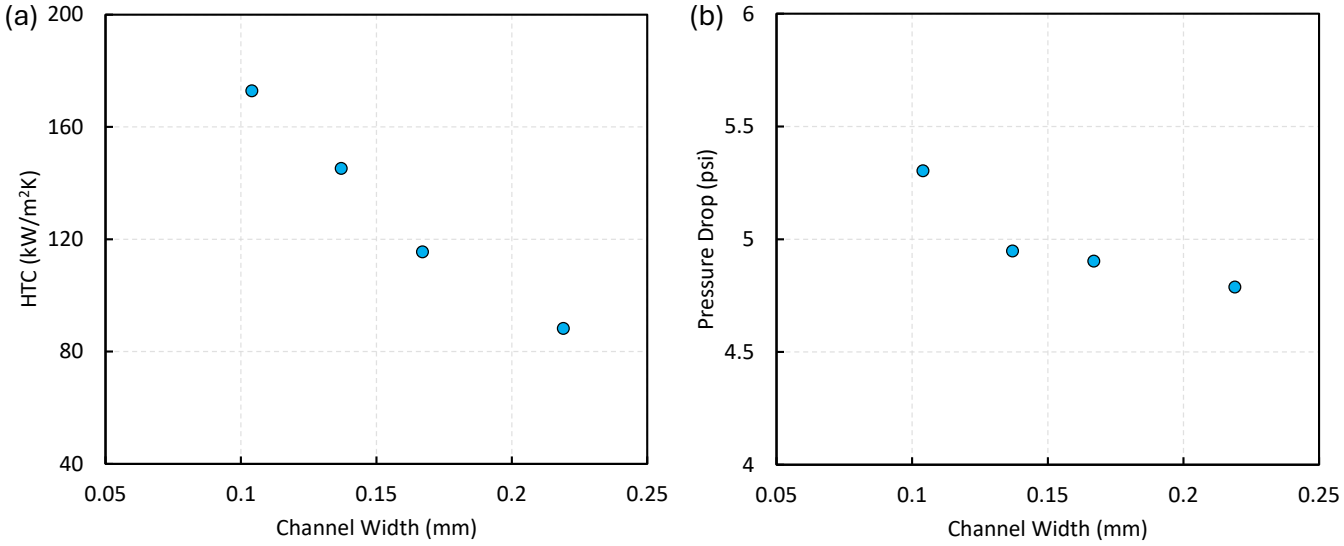


FIGURE 6: (a) Footprint HTC and (b) cold plate pressure drop as a function of channel width for CP group #3~6.

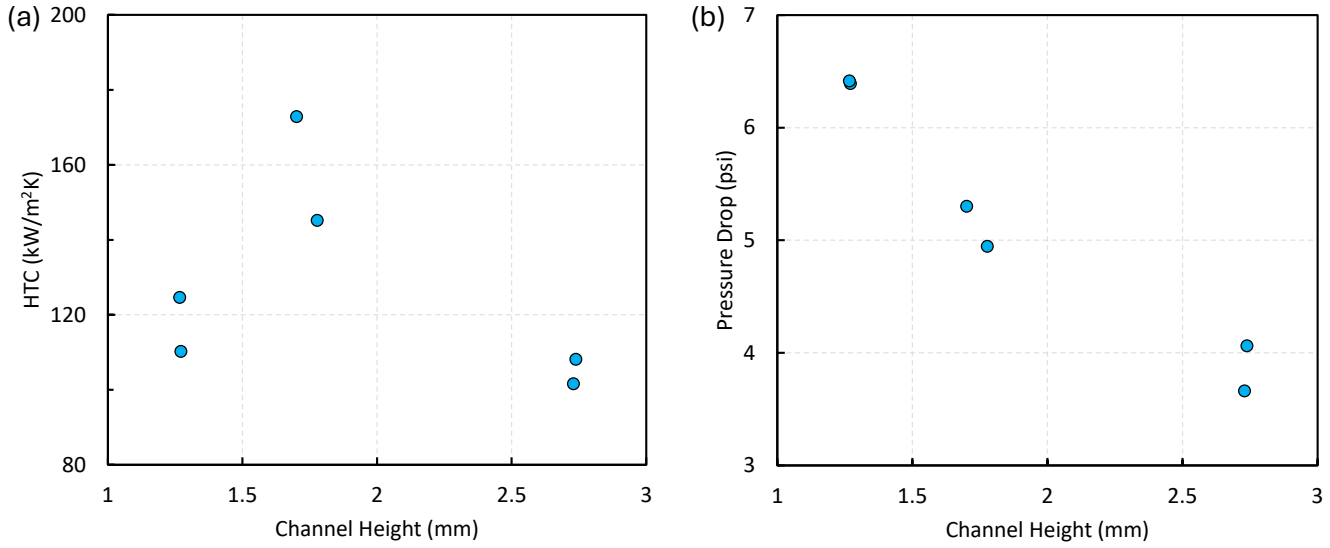


FIGURE 7: (a) Footprint HTC and (b) cold plate pressure drop as a function of channel height for CP group #1~4, 7, 8.

Copyright © 2026 by ASME

mm), to represent another group having narrow channels with width in the range of 0.1~0.15 mm and varying channel height. The maximum HTC and pressure drop as a function of channel height for these six cold plate samples are shown in Figure 7(a) and 7(b), respectively. Given the similar channel width, the pressure drop decreases with increasing channel height due to the increased cross-sectional area for flow. The HTC shows a non-monotonic trend, with a peak HTC achieved at intermediate channel height. This is consistent with model prediction reported in Ref. [20]. When the channel height is small, the channel wall has high fin efficiency so that increasing the channel height can effectively provide additional heat transfer area, resulting in increased footprint HTC. However, when the channel height is sufficiently large, further increasing the channel height only provides marginal heat transfer area enhancement due to depleted fin efficiency, but can cause unfavorable flow distribution within the high-aspect-ratio channel where the generated vapor stays near the base and liquid bypasses at the top, causing worsened overall heat transfer. The two competing effects render an optimal channel height for achieving the best heat transfer performance.

It is also noted that although not investigated in this work, the channel length can greatly impact microchannel thermohydraulic performance. It is expected that reducing the channel length will enhance HTC [20] and reduce pressure drop [22], especially at high heat flux conditions. In addition, by reducing the channel length, besides the heat transfer enhancement resulted from a single channel [20], the reduced channel pressure drop also alleviates the maldistribution and instability between parallel channels. Therefore, future study is needed to experimentally elucidate the effect of channel length, which will provide valuable insights for the design and implementation of skived-fin cold plates, including manifold microchannel configurations [12, 22].

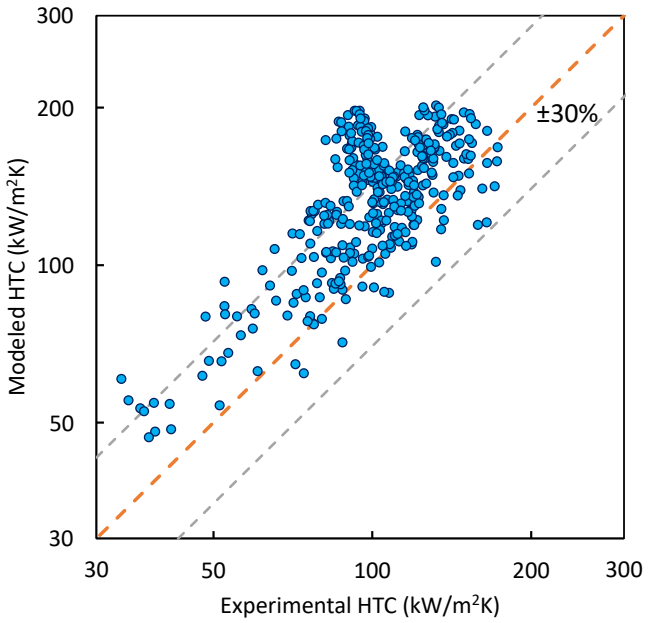


FIGURE 8: Comparison between model predicted and experimentally measured footprint HTC.

3.4. Comparison with Model

In our previous work [20], a model for microchannel cold plate was developed using correlations for both single-phase convection [23] and two-phase flow boiling [16]. The experimental results obtained from all eight cold plate samples in this work are collected into 363 steady-state data points. The working conditions and geometric parameters of these data points are used as inputs for the model to calculate the corresponding predicted HTCs. The comparison between predicted and experimental HTCs is plotted in Figure 8.

As discussed in previous sections, the model is mostly in qualitative agreement with experimental results. Figure 8 shows that quantitatively, the model generally overpredicts HTC slightly, which is evident from the upward shift of the data points from the diagonal. This can be attributed to the fact that the model assumes perfect thermofluidic distribution between the parallel channels whereas the realistic nonuniform distribution can cause performance degradation.

To evaluate the prediction accuracy of the model, the mean relative error (MRE), mean absolute relative error (MARE), and root mean square relative error (RMSRE) are defined as

$$\mathrm{MRE} = \frac{1}{N}\sum \frac{\mathrm{HTC}_{pre} - \mathrm{HTC}_{exp}}{\mathrm{HTC}_{exp}} \times 100\% \quad (6)$$

$$\mathrm{MARE} = \frac{1}{N}\sum \frac{\left|\mathrm{HTC}_{pre} - \mathrm{HTC}_{exp}\right|}{\mathrm{HTC}_{exp}} \times 100\% \quad (7)$$

$$\mathrm{RMSRE} = \sqrt{\frac{1}{N}\sum \left(\frac{\mathrm{HTC}_{pre} - \mathrm{HTC}_{exp}}{\mathrm{HTC}_{exp}}\right)^2} \times 100\% \quad (8)$$

where HTC_{pre} and HTC_{exp} are the model predicted and experimentally measured HTCs, respectively. The MRE, MARE, and RMSRE are obtained as 35.4%, 37.0% and 46.5%, respectively, for the data set of this work.

The MRE of 35.4% indicates that the original model overpredicts HTC on average. To improve the model accuracy with minimal efforts, a constant correction factor C can be applied to the model, i.e., $\mathrm{HTC}_{pre}^{*} = C \times \mathrm{HTC}_{pre}$. Minimization of MARE is set as the objective, and a parametric swept for the constant C is carried out. C = 0.727 is finally used in the corrected model, which yields an MRE, MARE, and RMSRE of -1.6%, 17.3%, and 21.5%, respectively. The small values of the errors indicate sufficient prediction accuracy of the corrected model. Nevertheless, for practical cold plate design and application, future work is encouraged to collect a larger set of data points with wider parameter ranges and working conditions, which can be used to fit into an application-specific correlation, or establish a higher-fidelity correction factor with a wider parametric coverage.

4. CONCLUSION

In this work, we conducted an experimental investigation on the thermohydraulic performance of skived-fin microchannel

Copyright © 2026 by ASME

cold plates for 2P DTC cooling using R515B. A TTV with a heated area of 26×35 mm^2 and a maximum power of 2000 W is used, corresponding to a maximum heat flux of 220 W/cm^2. Eight cold plates with different fin geometries are fabricated and tested under varying operating conditions. The findings include:

- The thermal resistance initially decreases with increasing exit quality due to the reduction of single-phase contribution and the development of boiling, and then increases at higher qualities due to potential dryout incipience or two-phase flow instabilities. A minimum area-specific case-to-fluid thermal resistance of <16 mm^2K/W is achieved, corresponding to a maximum footprint HTC of over 170 kW/m^2K.
- Under fixed heat flux conditions, the footprint HTC decreases with decreasing flow rate and increasing exit quality. A peak HTC is expected at an exit quality of approximately 0.2; however, this trend is not observed in the present study due to the limited range of tested flow rates.
- For a fixed channel height, the footprint HTC increases with decreasing channel width due to enhanced convective boiling. This can be attributed to stronger liquid film confinement within narrower channels in the convective boiling-dominated regime.
- For similar channel widths, the footprint HTC exhibits a non-monotonic dependence on channel height, increasing initially and then decreasing, indicating the existence of an optimal channel height. This behavior results from competing effects at larger channel heights: increased heat transfer area enhances performance, while unfavorable phase distribution leads to performance degradation.
- The pressure drop increases with both flow rate and heat load. Under fixed operating conditions, it decreases with increasing channel width and height due to reduced flow resistance.
- The experimental HTCs are compared with a previously developed model, showing good qualitative agreement. The model overpredicts HTC by ~30% on average, likely due to the assumption of uniform flow distribution. Future parametric experimental study is recommended to establish correlations or correction factors for improved model prediction accuracy in practical cold plate design.

ACKNOWLEDGEMENTS

The authors would like to thank Mackinnley Raulen and Kelly Pittinger for their support in system setup and experimental testing.

REFERENCES

[1] "Pumped 2P Refrigerant-Based Direct Liquid Cooling (DLC) Technology for Next Generation AI Clusters with High TDP Accelerators," OCP White Paper, 2025.

[2] Q. Wang, S. Ozguc, and R. W. Bonner, "Systematic Analysis of Thermal Resistances in Data Center Two-Phase Direct-to-Chip Cooling," in *Proc. ASME Int. Electron. Packag. Tech. Conf. Exhib.*, vol. 89299, p. V001T02A001, 2025.

[3] Q. Wang, S. Ozguc, and R. W. Bonner, "System-Level Thermal Analysis of Two-Phase Direct-to-Chip Cooling for Data Centers with Chilled Facility Water," *J. Electron. Packag.*, vol. 148, no. 4, p. 040904, 2026.

[4] H. J. Cho, D. J. Preston, Y. Zhu, and E. N. Wang, "Nanoengineered materials for liquid–vapour phase-change heat transfer," *Nature Rev. Mater.*, vol. 2, no. 2, p. 16092, 2017.

[5] X. Liu *et al.*, "Enhancing Liquid–Vapor Phase-Change Heat Transfer with Micro/Nano-Structured Surfaces," *ACS Nano*, vol. 19, no. 10, pp. 9513–9589, 2025.

[6] D. Kulkarni, J. Gulick, J. King, B. Jarrett, P. George, and Y. Feldman, "Thermal performance of common cold plate for pumped single-and two-phase direct liquid cooling for next generation high power server processors," in *Proc. ASME Int. Electron. Packag. Tech. Conf. Exhib.*, vol. 88469, p. V001T02A013, 2024.

[7] Q. Wang, D. P. Kulkarni, R. W. Bonner, and J. C. Gulick, "Universal Direct-to-Chip Cold Plates for Single- and Two-Phase Cooling," in *OCP Global Summit Future Technol. Symp.*, 2024.

[8] Q. Wang, S. Ozguc, A. Narayanan, and R. W. Bonner, "A Server-Level Test System for Direct-To-Chip Two-Phase Cooling of Data Centers Using a Low Global Warming Potential Fluid," in *Proc. 23rd IEEE Intersoc. Conf. Thermal Thermomech. Phenom. Electron. Syst. (ITherm)*, 2024.

[9] A. Narayanan, Q. Wang, S. Ozguc, and R. W. Bonner, "Investigation of Server Level Direct-to-Chip Two-Phase Cooling Solution for High Power GPUs," in *Proc. ASME Int. Electron. Packag. Tech. Conf. Exhib.*, vol. 88469, p. V001T02A009, 2024.

[10] Q. Wang, A. Narayanan, S. Ozguc, J. D. Moore, and R. W. Bonner, "Performance Comparison of R1233zd(E) and R515B for Two-Phase Direct-to-Chip Cooling," in *Proc. 24th IEEE Intersoc. Conf. Thermal Thermomech. Phenom. Electron. Syst. (ITherm)*, 2025, pp. 1–8.

[11] Q. Wang and R. W. Bonner, "High-Performance Two-Phase Cooling under Different Cold Plate Orientations," in *OCP EMEA Summit Future Technol. Symp.*, 2025.

[12] S. Ozguc, Q. Wang, A. Narayanan, J. Moore, and R. W. Bonner, "Design Optimization of Manifold Integrated Skived Cold Plates for Two-Phase Flow-Boiling," in *Proc. 41st Semi. Thermal Meas. Model. Manage. Symp. (SEMI-THERM)*, 2025.

[13] S. G. Kandlikar, "Fundamental issues related to flow boiling in minichannels and microchannels," *Exp. Thermal Fluid Sci.*, vol. 26, no. 2–4, pp. 389–407, 2002.

[14] J. R. Thome, "State-of-the-art overview of boiling and two-phase flows in microchannels," *Heat Transfer Eng.*, vol. 27, no. 9, pp. 4–19, 2006.

Copyright © 2026 by ASME

[15] S. G. Kandlikar, "History, advances, and challenges in liquid flow and flow boiling heat transfer in microchannels: a critical review," *ASME J. Heat Transfer*, vol. 134, no. 3, p. 034001, 2012.

[16] S. M. Kim and I. Mudawar, "Universal approach to predicting saturated flow boiling heat transfer in mini/micro-channels–Part II. Two-phase heat transfer coefficient," *Int. J. Heat Mass Transfer*, vol. 64, pp. 1239–1256, 2013.

[17] S. G. Kandlikar, "Heat transfer mechanisms during flow boiling in microchannels," *ASME J. Heat Transfer*, vol. 126, no. 1, pp. 8–16, 2004.

[18] H. Qiu *et al.*, "Scalably etched large footprint copper cold plates for high-power dissipation in data centers using R1233zd(E)," *Int. J. Heat Mass Transfer*, vol. 256, p. 127938, 2026.

[19] Q. Wang, S. Ozguc, and R. W. Bonner, "A Practical Metric for Cold Plate Thermal Performance in Two-Phase Direct-to-Chip Cooling," in *Proc. 41st Semi. Thermal Meas. Model. Manage. Symp. (SEMI-THERM)*, 2025.

[20] Q. Wang, T. A. Whitaker, A. Narayanan, S. Ozguc, J. D. Moore, and R. W. Bonner, "Thermohydraulic Modeling of Microchannel Cold Plates for Two-Phase Data Center Cooling," in *Proc. 25th IEEE Intersoc. Conf. Thermal Thermomech. Phenom. Electron. Syst. (ITherm)*, 2026.

[21] S. M. Kim and I. Mudawar, "Universal approach to predicting saturated flow boiling heat transfer in mini/micro-channels–Part I. Dryout incipience quality," *Int. J. Heat Mass Transfer*, vol. 64, pp. 1226–1238, 2013.

[22] H. Wang, Y. Qiu, J. Carter, J. McGuffin-Cawley, and C. R. Kharangate, "Effects of heating orientation on flow boiling in copper manifold microchannel heat sinks," *Exp. Thermal Fluid Sci.*, vol. 169, p. 111553, 2025.

[23] S. G. Kandlikar, S. Garimella, D. Li, S. Colin, and M. R. King, *Heat Transfer and Fluid Flow in Minichannels and Microchannels*. Elsevier, 2006.

Copyright © 2026 by ASME